

# A Simplified Method of Wind Speed Estimation Using the Inertial Measurement Unit on a Quad-Copter UAV

**Dr. Phillip B. Chilson, Austin Dixon**

Advanced Radar Research Center, University of Oklahoma, Norman, 73072-7307, United States

**Abstract.** This paper presents a simplified method of estimating wind speed with a quad-copter unmanned aerial vehicle using data from its onboard inertial measurement. The method presented neglects the need for measured drag coefficients via wind tunnel by introducing an experimentally determined coefficient based on orientation of the aircraft. A field experiment was conducted where the copter hovered near an Oklahoma Mesonet tower for verification. Results of the experiment are presented against data from the Mesonet tower to show application of the determined coefficients.

## 1. Introduction

Local wind vector is a critical variable in meteorological observation and has been sampled through various methods over the last several decades. Development of Unmanned Aerial Vehicle (UAV) technology in recent years has brought forth the idea of using UAVs for measuring various meteorological variables including wind. Cup anemometers and wind vanes are sufficient methods for mesoscale measurement techniques but are generally limited to their mounted locations such as Oklahoma Mesonet stations (Brock and Crawford et. Al. 1994). Unmanned aerial vehicles (UAV) provide a method of mobile measurement that allows for sampling of the atmosphere in a large range of altitudes not possible with other mobile measurement systems such as the so-called “Mobile Mesonet” vehicles (Straka et. Al. 1996). While a Mobile Mesonet provides a method of portable measurement, observations of this nature are limited to near-surface data.

The method used to obtain wind speed in this paper is the interpretation of data recorded by the Inertial Measurement Unit onboard a UAV. Using the onboard IMU to estimate the wind speed allows for no additional hardware requirements outside of what is needed to fly the aircraft. This allows for other meteorological sensors to be placed on the copter without extensive payload requirements. An IMU also provides data with extremely high temporal resolution (100 Hz and higher) due to the need for rapid response from the onboard autopilot for autonomous functions. Measuring the local wind speed with these UAV is critical for high spatial and temporal resolution mobile measurements that are not possible with operational measurement stations or Mobile Mesonet systems. Some applications of these measurements could be for observations of micro-scale, storm-scale and mesoscale wind fields, as well as boundary layer flows, and aerosol transport.

Obtaining the wind speed from an IMU requires thorough understanding of how these data are recorded onboard the UAV. We will first provide an overview of related work. We then provide a description of the quad-copter UAV and the onboard autopilot system used in this experiment. We then provide a description of how the wind speed is obtained. The approach used in this paper to obtain the wind speed is similar to that of Neumann and Bartholmai but uses estimated drag coefficients as opposed to values determined in a wind tunnel. This paper will provide a method of determining drag coefficients based on comparisons between estimated and observed wind speeds. Additionally, experiments and results are presented where the UAV was hovering in an open field at the Kessler Atmospheric and Ecological Field Station (KAEFS) in Purcell, Oklahoma. Flights were conducted near the Washington Oklahoma Mesonet station at KAEFS to provide validation of these measurements. The predominant sensor on the Mesonet tower that was referenced in this experiment is an R.M. Young Wind Monitor (will be referred to as Wind Monitor from this point forward), which sits at 10 meters on top of the tower. See Brock and Richardson et. Al. for more information on the Mesonet stations. Finally, we present our conclusions as well as provide some direction for future works.

## 2. Related Works

Some previous experiments have attempted to use UAVs to measure the local wind vector through various methods. Some of the methods include ground-based microphone communication (Rogers and Finn 2013) and also interpretation of onboard inertial measurement unit (IMU) data (Neumann and Bartholmai 2015). Other methods have involved using Pitot tubes with fixed-wing aircraft (Molnar et. Al. 2010) as well as the use of optical flow sensors onboard a UAV (Rodriguez et. Al. 2007). The method of ground-based microphone communication can provide accurate data but may be limited by the number of ground stations in the vicinity of the UAV. Pitot tubes are applicable with fixed wing aircraft but are not useful on a quad-rotor copter due to fluctuations in “inclination angle” as well as low airspeeds (Neumann and Bartholmai 2015). In 2010, Langleann et. Al. provided a method of measuring wind velocity on a fixed wing aircraft through relation of the airspeed and GPS measured velocity of the vehicle. This method showed promising results but involved extensive derivation and use of the equations of motion for a vehicle in flight. Marino et. Al. explored the possibility of using a relationship between the rotation rates of the forward and rear rotors and the wind speed in 2015. It was found that it was possible to derive an accurate relationship, but it was only useful over a very small measurement space and therefore impractical. That same year, Neumann and Bartholmai determined that many of the previous experiments that aimed to measure wind speed via UAV relied on aerodynamic models. They stated that many of these models required “measurability of the UAV’s full state” which often requires further determination before wind experiments can be conducted.

The approach of using the onboard IMU for wind speed estimation negates the need for onboard sensors and understanding of complex aerodynamic models. By using IMU data only, payload capacity is free to be used by other meteorological

or related sensors. In this paper, we present a method of obtaining the wind speed that requires only a working knowledge of vector calculus and basic IMU data.

### 3. Wind Speed Estimation Using the Pixhawk

The wind speed estimation in this experiment focuses predominantly on the pitch ( $\theta$ ), roll ( $\phi$ ), and yaw ( $\lambda$ ) angles of the copter. Pitch and roll are recorded through the copter's IMU and yaw is determined by the copter's orientation to the North Pole based on GPS, and a magnetometer. The coordinate system is the aviation-based convention of "north-east-down" in which the positive z-axis points into the ground. Neumann and Bartholmai provided an illustration for a copter's local coordinate system in **Fig. 1**. Eq. 1 shows how the (rotated) unit vectors of pitch and roll ( $\vec{e}_\theta$ ,  $\vec{e}_\phi$ , respectively) can be determined (Neumann and Bartholmai 2015).

$$\vec{e}_\theta = \begin{pmatrix} \cos \theta \\ 0 \\ -\sin \theta \end{pmatrix}, \vec{e}_\phi = \begin{pmatrix} 0 \\ \cos \phi \\ \sin \phi \end{pmatrix} \quad (1)$$

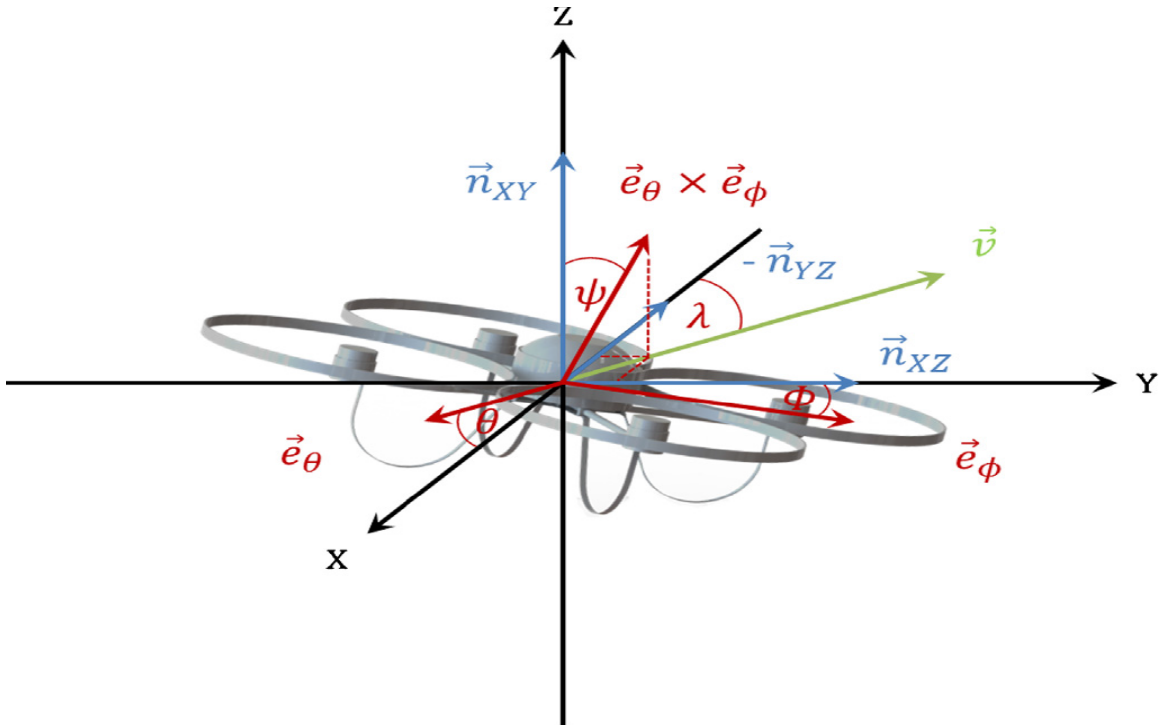


**Fig. 1.** Illustration of the copter's local coordinate system provided by Neumann and Bartholmai 2015. The x-axis is considered the viewing direction of the copter. The flight vector  $\vec{v} = (r_v, r_\theta)$  can be simplified to  $r_v$  since only the speed is being considered.

The vector  $\overrightarrow{n_{XY}}$  is normal to the XY-plane;  $\overrightarrow{n_{XZ}}$  is normal to the XZ-plane, etc. Here, we introduce what Neumann and Bartholmai refer to as the "inclination angle" ( $\psi$ ). This inclination angle is the deflection of the copter from the vector  $\overrightarrow{n_{XY}}$ , which is calculated as shown in Eq. 2.

$$\psi = \cos^{-1} \left( \frac{\overrightarrow{n_{XY}} \cdot (\overrightarrow{e_\theta} \times \overrightarrow{e_\phi})}{|\overrightarrow{n_{XY}}| \cdot |\overrightarrow{e_\theta} \times \overrightarrow{e_\phi}|} \right) \quad (2)$$

Neumann and Bartholmai call this the “inverse scalar product from the cross product of the (rotated) unit vectors” in Eq. 1, where  $\overrightarrow{n_{XY}} \cdot \overrightarrow{n_{XY}} = (0, 0, 1)$  is the unit normal vector to the XY-plane. Once the angle  $\psi$  has been determined it can be used to calculate the drag force  $F_D$ .

$$F_D = m \cdot g \cdot \tan \psi \quad (3)$$

where  $m$  is the mass of the copter and  $g$  is the acceleration due to gravity (both assumed to be constant). The drag force is then used to calculate the flight speed  $r_v$ .

$$r_v = \sqrt{\frac{2 \cdot F_D}{\rho \cdot A_{proj} \cdot C_d}} \quad (4)$$

where  $\rho$  is density of air (assumed to be constant),  $A_{proj}$  is the projection of the wind onto the surface of the copter, and  $C_d$  is the drag coefficient. The drag coefficient and projected area vary dependent on the orientation of the copter (yaw angle  $\lambda$ ) to the wind. Neumann and Bartholmai used a wind tunnel and a 3D CAD program to calculate accurate values of  $C_d$  and  $A_{proj}$ , respectively. In this experiment we combine  $m$ ,  $g$ ,  $\rho$ ,  $C_d$ , and  $A_{proj}$  and introduce the variable  $\alpha$ , which we will call the “rotation coefficient.” The rotation coefficient is based on the idea that the copter experiences different drag forces based on yaw angle with respect to the wind. It is multiplied outside of the radical (Eq. 5) to amplify the value of the flight speed and is determined experimentally. Examples of this amplification and how the coefficient is determined will be shown later.

$$r_v = \alpha \sqrt{2 \cdot F_D} \quad (5)$$

Since the mass of the copter and acceleration due to gravity are now inside of the rotation coefficient, we are left with a simpler equation for the drag force.

$$F_D = \tan \psi \quad (6)$$

Substituting this into (Eq. 5) gives the final resulting equation for the flight speed.

$$r_v = \alpha \sqrt{2 \cdot \tan \psi}$$

Since the copter is hovering in one location throughout the experiment the flight speed is assumed to be equivalent to wind speed. In essence, this assumes that a copter flying at 10 meters per second in no wind would be under the same conditions as a copter hovering in winds of 10 meters per second.

#### 4. Quad-Copter UAV

The UAV used in this experiment is the IRIS+ from 3DRobotics. It is a micro quad-rotor copter with a payload capacity of 400g, and can reach speeds of around 17 meters per second. It is equipped with 4 9.5-inch rotors, which are powered by 950 KV brushless motors. Two of the rotors spin clockwise and two spin counterclockwise for stability. The IRIS+ can hover reliably in wind speeds up to 8 meters per second; the copter begins to have difficulty holding altitude once this value is exceeded. The maximum flight time of the copter is 16 minutes with a 5100 mAh LiPo battery. The onboard flight controller is a 3DRobotics Pixhawk autopilot system, which uses an IMU to maintain position when the copter encounters wind. The data from this IMU is what will be used to analyze the wind vector in this paper. The copter and respective Pixhawk are similar to the onboard sensors used by Neumann and Bartholmai. Neumann and Bartholmai used an AirRobot AR100-B “plus” frame quad-copter, whereas the IRIS+ is a “V” frame quad-copter (Fig. 2). More information on frame types can be found on the ArduPilot page provided below (ArduPilot Dev.)



(a)



(b)



(c)

**Fig. 2.** Front (a), side (b), and top (c) views of the 3DR IRIS+. The PVC elbows on the underside of the copter serve as protective shields for other meteorological sensors not used in this paper.

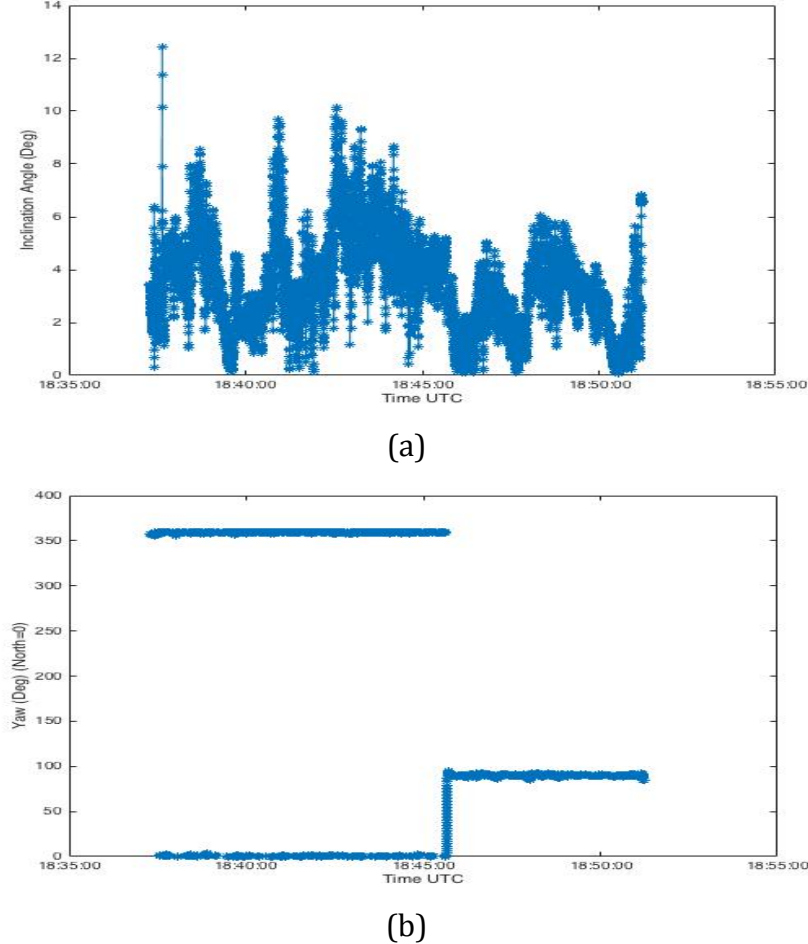
The Pixhawk is a next generation 32-bit open-source autopilot system with a Cortex M4 processor. It contains a three-dimensional accelerometer and attitude-rate sensor. An onboard global positioning system (GPS), magnetometer, and barometer are used to determine the copters altitude as well as enhance the performance of the IMU. Autonomous flight is performed through communication with the ArduPilot Mission Planner ground control station via MAVLink (Micro Aerial Vehicle Link) antenna, which is connected to the Pixhawk. The Pixhawk and MAVLink antenna communicate at a frequency of 915 MHz in the US and 433 MHz in the rest of the world. The IRIS+ can also be flown manually using any PPM compatible RC controller. Data between the Pixhawk and ground station can include flight plan information as well as data from the onboard sensors. This data is also stored on a Micro SD card onboard the Pixhawk for post-flight analysis. The data from the Pixhawk contains the IMU information, which is the basis for this paper. More information can be found about the Pixhawk autopilot system on the webpage provided below (PX4 Autopilot).

## 2.1 Experimental Conditions and Flight Plans

Several flights were conducted in close proximity ( $\sim 10$  meters) to the Washington Mesonet tower at KAEFS. The copter was programmed to takeoff to an altitude of 10 meters to be level with the Wind Monitor for comparison. Once the altitude of 10 meters was reached the copter hovered at this altitude indefinitely until the battery voltage was low. Flights were conducted with the copter initially facing into the wind (north in this case) for 8 minutes and rotating  $90^\circ$  to the east for the remainder (approximately 8 minutes). This was done to test the variation of the rotation coefficient  $\alpha$ . The wind direction was estimated based on the orientation of the Wind Monitor. Wind conditions ranged between 2 and 6 meters per second during the experiment.

### 3. Results

#### 3.1 Inclination Angle



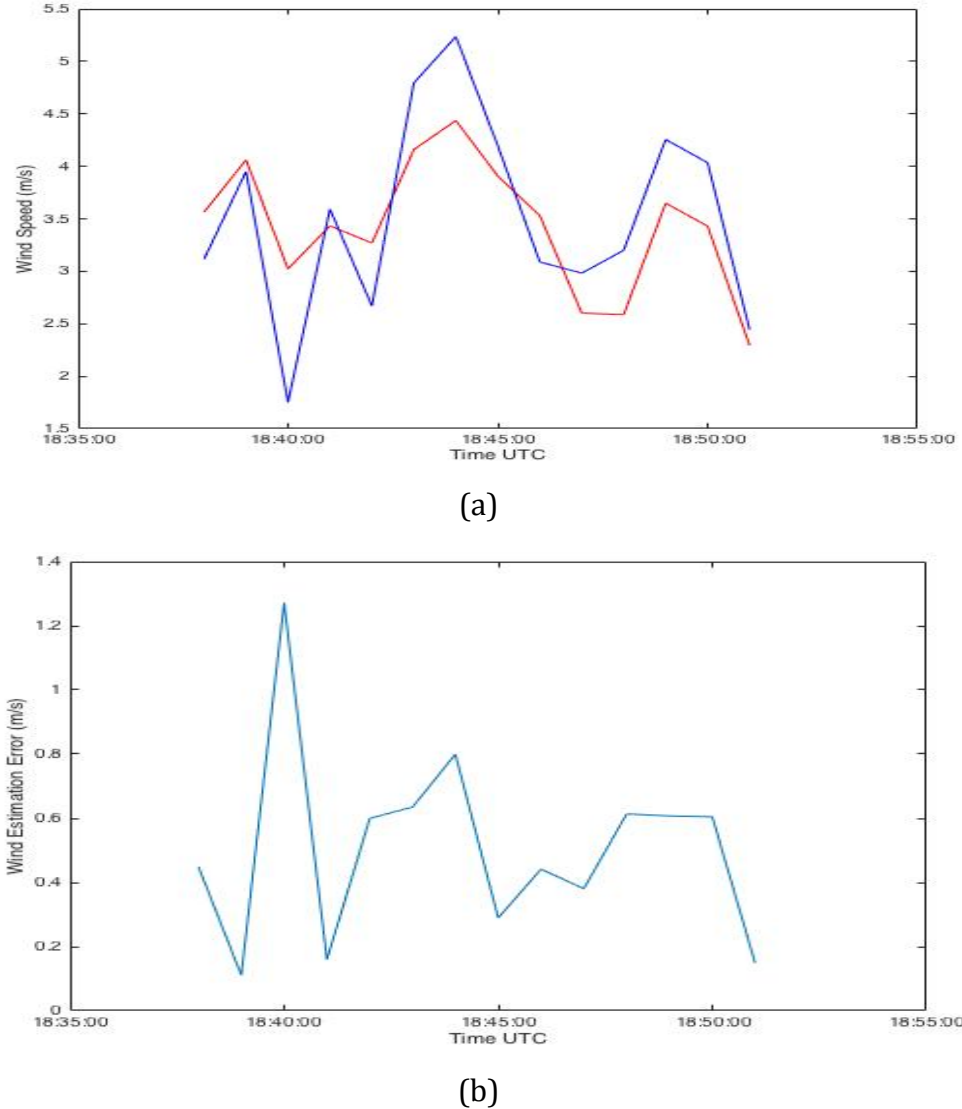
**Fig. 3.** Observed inclination angle  $\psi$  (a) from a hovered flight at 10 meters with two orientations ( $0^\circ$  and  $90^\circ$ ) as shown by the yaw angle (b).

Fig. 3 shows the results from the experiment for the inclination angle and the corresponding yaw angle. The copter rotated  $90^\circ$  from north at approximately 1846 UTC (Fig. 3(b)). In Fig. 3(a) the inclination angle decreases overall after this rotation. Therefore, the orientation of the copter plays a key role in inclination angle. This is expected since the rotation of the copter decreases the projected surface area of the wind based on its shape (see Fig. 2). This indicates that the copter will measure different wind values for different rotation angles with a constant coefficient.

#### 3.2. Wind Speed Estimation and Applying the Rotation Coefficient

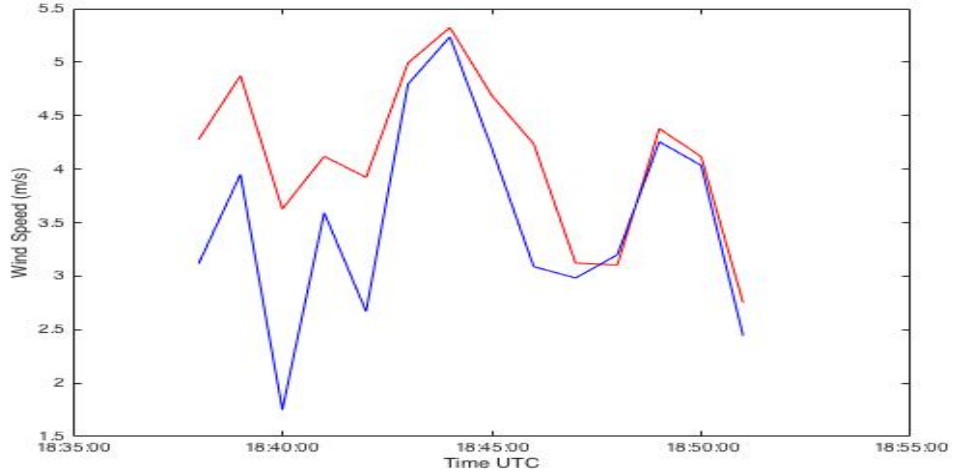
As described before, the rotation coefficient  $\alpha$  must be determined experimentally by using a reference sensor (Wind Monitor in this case). To do this,

$r_v$  is plotted against the reference sensor and a value of  $\alpha$  is chosen that matches the copter data with the observed data. In this experiment,  $\alpha$  was determined to be  $\sim 10$  for a yaw angle of  $0^\circ$  (Fig. 4) and  $\sim 12$  for a yaw angle of  $90^\circ$  (Fig. 5). Since a yaw angle of  $90^\circ$  results in lower inclination angles we expect  $\alpha$  to be higher. This same line of reasoning explains why a yaw of  $0^\circ$  requires a lower value of  $\alpha$ .

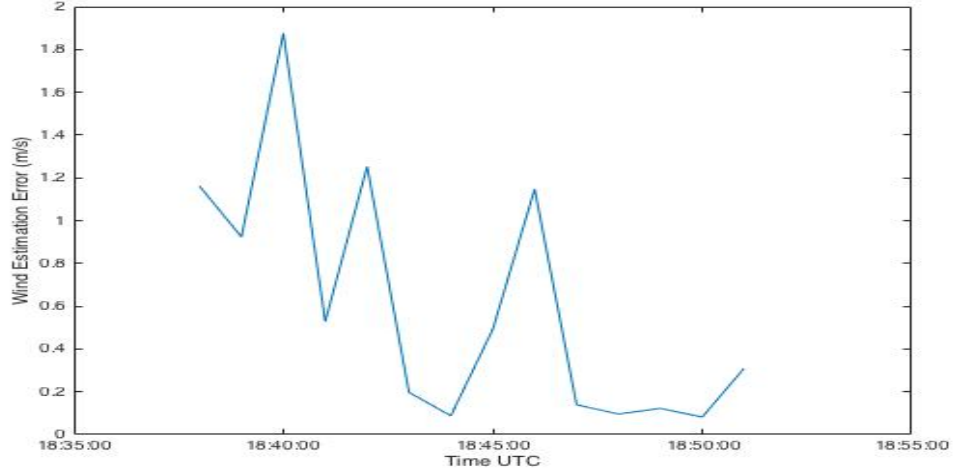


**Fig. 4.** Estimated wind speed (red) plotted against the corresponding Mesonet data (blue) using a rotation coefficient of 10 (a) and error between the estimated wind and Mesonet tower (b).

When using  $\alpha = 10$ , the data that corresponds to a yaw angle of  $0^\circ$  (see Fig. 3) is in general agreement with the Mesonet tower. Error between the copter and Mesonet is about 0.5 meters per second on average. Once the copter begins to rotate, the data is underestimated as expected. In both cases, the overall trend of the data is also in excellent agreement.



(a)



(b)

**Fig. 5.** Estimated wind speed (red) plotted against the corresponding Mesonet data (blue) using a rotation coefficient of 12 (a) and error between the estimated wind and Mesonet tower (b).

When using  $\alpha = 12$ , the data corresponding to a yaw angle of  $90^\circ$  (see Fig. 3) is again in generally good agreement with the Mesonet tower. Error for the  $90^\circ$  data is lower than error for the  $0^\circ$  data in Fig. 4 and nearly zero in a significant portion of the last 5 minutes of flight. We can see that the data previously matched with the Mesonet in Fig. 4 is now overestimating with the new coefficient, as expected. With both coefficients there was a notable fluctuation in the trend line as the copter rotated between  $0^\circ$  and  $90^\circ$  that led to overestimation. More investigation of how inclination angle behaves during rotation will likely be needed in the future.

## **4. Summary and Conclusions**

A method for obtaining the wind speed from a UAV's onboard IMU has been presented. This approach was validated in field experiments against data from an Oklahoma Mesonet tower. The method presented negates the need for other onboard sensors or extensive application of flight motion equations to calculate the wind speed. A new equation has been introduced that does not require rigorous calculation of a drag coefficient or projected area for a UAV, making this method more accessible.

Rotation coefficients were determined experimentally for the UAV based on comparison with data from an Oklahoma Mesonet. It was discovered that this coefficient varies based on orientation of the UAV to the wind. Plots were shown that illustrate the results from two different orientations with respective coefficients applied. The results show that a reasonable estimation of the wind can be calculated with a quad-copter UAV.

Future work should include also the determination of more rotation coefficients and investigating how to apply them without the need for multiple plots. One approach to this could be collecting data with a wide range of yaw angles, determining their coefficients, and then applying them to the data with the corresponding yaw in one plot. Future work should also investigate the error in the wind speed estimations associated with the rotation of the UAV. It is possible that this rotation error will be resolved with further investigation of rotation coefficients. Estimating the wind with a moving UAV is also a possibility of future study. It is possible that this could also be done with the IMU, but further investigation of this data is needed.

## **Acknowledgements**

The authors thank the Kessler Atmospheric and Ecological Field Station for participation in the experiments, as well as participating colleagues from the OU Advanced Radar Research Center.

## References

- Ardupilot Development Team. "Advanced MultiCopter Design." *Advanced MultiCopter Design — Copter Documentation*. Web. 02 May 2016. <<http://ardupilot.org/copter/docs/advanced-multicopter-design.html>>.
- Brock, Fred V., Kenneth C. Crawford, Ronald L. Elliott, Gerrit W. Cuperus, Steven J. Stadler, Howard L. Johnson, and Michael D. Eilts. "The Oklahoma Mesonet: A Technical Overview." *J. Atmos. Oceanic Technol. Journal of Atmospheric and Oceanic Technology* 12.1 (1995): 5-19. Web.
- Langelaan, Jack, Nicholas Alley, and James Niedhoefer. "Wind Field Estimation for Small Unmanned Aerial Vehicles." *AIAA Guidance, Navigation, and Control Conference* (2010). Web.
- Marino, Matthew, Alex Fisher, Reece Clothier, Simon Watkins, Samuel Prudden, and Chung Sing Leung. "An Evaluation of Multi-Rotor Unmanned Aircraft as Flying Wind Sensors." *International Journal of Micro Air Vehicles* 7.3 (2015): 285-300. Web.
- Molnar, A., and D. Stojcsics. "New Approach of the Navigation Control of Small Size UAVs." *19th International Workshop on Robotics in Alpe-Adria-Danube Region (RAAD 2010)* (2010). Web.
- Neumann, Patrick P., and Matthias Bartholmai. "Real-time Wind Estimation on a Micro Unmanned Aerial Vehicle Using Its Inertial Measurement Unit." *Sensors and Actuators A: Physical* 235 (2015): 300-10. Web.
- PX4 Autopilot. "Pixhawk Autopilot." *Pixhawk Flight Controller Hardware Project*. Web. 02 May 2016. <<https://pixhawk.org/modules/pixhawk#specifications>>.
- Rodriguez, Andres, Evan Andersen, Justin Bradley, and Clark Taylor. "Wind Estimation Using an Optical Flow Sensor on a Miniature Air Vehicle." *AIAA Guidance, Navigation and Control Conference and Exhibit* (2007). Web.
- Rogers, Kevin, and Anthony Finn. "Three-Dimensional UAV-Based Atmospheric Tomography." *J. Atmos. Oceanic Technol. Journal of Atmospheric and Oceanic Technology* 30.2 (2013): 336-44. Web.
- Straka, Jerry M., Erik N. Rasmussen, and Sherman E. Fredrickson. "A Mobile Mesonet for Finescale Meteorological Observations." *J. Atmos. Oceanic Technol. Journal of Atmospheric and Oceanic Technology* 13.5 (1996): 921-36. Web.